C.P. No. 572

C.P. No. 572

MINISTRY OF AVIATION

AERONAUTICAL RESEARCH COUNCIL

CURRENT PAPERS

Free-Flight Measurements of Control Effectiveness on Three Wing Planforms at Transonic Speeds

by

J. B. W. Edwards

LONDON: HER MAJESTY'S STATIONERY OFFICE

1961

FOUR SHILLINGS NET

U.D.C. No. 533.694.51:533.693.1:533.692.1:533.6.011.35:533.6.055:[Ae]RAE 102

C.P. No. 572

March, 1961

FREE-FLIGHT MEASUREMENTS OF CONTROL EFFECTIVENESS ON THREE WING PLANFORMS AT TRANSONIC SPEEDS

by

J. B. W. Edwards

SUMMARY

The rolling effectiveness of a series of flap and tip controls has been measured by means of rocket-propelled test vehicles, over the Mach number range 0.8-1.3. The controls were attached to three basic planforms all of nett aspect ratio 2.83 and having R.A.E. 102 aerofoil sections. Each planform was flown with four different controls and two values of thickness:chord ratio (0.06 and 0.075).

Results for all the configurations are given in terms of the ratio ℓ_ξ/ℓ_p: for certain wing:control combinations it was possible to isolate the aileron-effectiveness derivative ℓ_ξ.

Previously issued as R.A.E. Tech. Note No. Aero.2747 - A.R.C. 22,967.

LIST OF CONTENTS

LIST OF TABLES

LIST OF ILLUSTRATIONS

LIST OF ILLUSTRATIONS (Cont'd.)

1 INTRODUCTION

In 1953 Taylor and Thomas of the Royal Aircraft Establishment put forward a minimal experimental programme on wing mounted flap and tip controls which was intended to reveal the separate effects of such variables as wing sweepback, taper ratio, thickness:chord ratio and control geometry. In the event very little of the programme ever came to being but a number of free-flight rolling tests were made to measure rolling effectiveness and roll-damping.

The results on roll-damping were reported in Ref.1. The results on effectiveness are presented here for the record with the minimum of discussion. The programme was based on three related planforms, each having an aspect ratio of 2.83. Planforms A and B each had a taper ratio of 0.333 but differed in sweepback; planform A having a leading-edge sweepback of 28° and planform B, $53\frac{1}{2}^{\circ}$. Planform C was a cropped delta planform of taper ratio 0.086 and a leading-edge sweepback of 50°.

A total of 16 test vehicles were flown, four of each planform with flap controls and a further four with all-moving tip controls. Full details of all the vehicles are given in Tables 1 and 2 and they are illustrated in Figs.1-3.

2 DESCRIPTION OF THE MODELS

Typical test vehicles incorporating each planform are illustrated in Fig.3 and the leading dimensions and parameters of all 16 models flown are given in Figs.1 and 2 and Table 1. The models fall into four groups; there were four models of each planform with trailing-edge flap controls forming three of the groups, plus four models with wing-tip controls in the fourth group. Of the four models of each planform, three were of 6% thickness:chord ratio with aileron-chord to wing chord ratios, c_{ζ}/c, of 0.1, 0.25 and 0.4, and the fourth model was $7\frac{1}{2}\%$ thick with $c_{\zeta}/c = 0.25$. The four tip-control models were all 6% thick and the control was the outboard quarter of the span in each case. All wings were of R.A.E. 102 section along wind direction; thus the smaller chord controls ($c_{\zeta}/c = 0.1, 0.25$) were of simple wedge section.

The body of each model was made of a resin-bonded paper-based tube fitted round the 5" diameter boost motor. The method of construction of the wings was changed several times as the programme developed, generally with a view to increasing the stiffness in order to reduce the magnitude of the aeroelastic corrections that had to be applied. Details of the various methods employed are listed in Table 2. Each vehicle consisted of three wings symmetrically fitted round the circumference of the body.

The ogival nose was made of perspex and contained the telemetry equipment by which the rolling motion of the model is measured in flight. Further details of similar models are given in Ref.2.

3 THE EXPERIMENTAL METHOD

A full description of the experimental method is given in Ref.2. Before flight, measurements are made of the model's moment of inertia in roll and of the elastic properties of the wing; these are needed to evaluate the corrections applied to the results for roll acceleration and aeroelastic deformation respectively.

The model is boosted to a maximum Mach number of between 1.3 and 1.4 by its integral rocket motor and then coasts down through the transonic speed range. It is during the coasting phase of the flight that measurements are made.

When the ailerons are deflected and the vehicle is rolling steadily, the rolling moment from the ailerons is just balanced by the damping-in-roll. Thus we have

$$L_\xi \cdot \xi + L_p \cdot \bar{p} = 0$$

or in non-dimensional terms

$$\ell_\xi \cdot \rho V^2 S \cdot \frac{b}{2} \cdot \xi + \ell_p \cdot \rho V S \left(\frac{b}{2}\right)^2 \cdot \bar{p} = 0$$

or

$$\ell_\xi = -\ell_p \cdot \frac{\bar{p}b}{2V\xi}$$

where $\bar{p}$ is the steady-rolling velocity and ξ the aileron-deflexion angle. The quantities $\bar{p}$ and V are measured by means of the telemetry equipment and radio Doppler, respectively, during flight. Thus $\bar{p}b/2V\xi$ can be calculated and from this the derivative ℓ_ξ using the values of ℓ_p from Ref.1 (shown in Table 3). The expressions above assume that the rate of roll is constant, but this is not strictly true. For this investigation however the inertia correction terms due to rolling acceleration proved to be very small indeed and were ignored.

Graphs of velocity and Mach number against time and of rate of roll against time for a typical vehicle (Model number 8) are shown in Figs.4a and 4b.

4 AEROELASTIC CORRECTIONS

The results for $\bar{p}b/2V\xi$ have been corrected for the loss in rolling moment due to aeroelastic deformation of the wing and control. This has been done using the iterative process due to Broadbent (Ref.3) for both subsonic and supersonic speeds. At transonic speeds where it was not possible to get accurate estimates of the aerodynamic derivatives required, the value of the correction factor, X, which is the ratio of the rolling effectiveness of the flexible wing, to the rolling effectiveness of the rigid wing, was assumed to vary linearly between the computed subsonic and supersonic values at M = 0.9 and 1.1, respectively. The values of X used are plotted in Fig.12. For planform A the corrections are small (< 10%); for planforms B and C they were larger but for the most part did not exceed 30% and were never over 40%. The correction factors for the tip control models were very small indeed because the lift from the tip has only a very small twisting moment acting on the wing; flexibility corrections were therefore deemed unnecessary.

5 RESULTS AND DISCUSSION

The rolling effectiveness curves, $\bar{p}b/2V\xi$ against Mach number, are plotted in Figs.5-7 for each of the models. For convenience in comparison the 16 results have been split up into groups as follows:- the models with t/c of 6% and 7½% and $c_\xi/c = 0.25$ of all three planforms in Fig.5; the three models with t/c of 6% of each planform and varying c_ξ/c ratio in Fig.6, and the four models with tip controls in Fig.7. All the results

were obtained under conditions of zero lift and at a Reynolds number of about 9×10^6 at M = 1 for planforms A and B, and 6×10^6 at M = 1 for planform C, based on the aerodynamic mean chord.

5.1 Thickness effects

Fig.5 illustrates the changes in rolling effectiveness caused by a change in thickness:chord ratio for each of the three planforms.

Planform A shows a sudden drop in aileron effectiveness from subsonic to supersonic speeds which is characteristic of flap controls. On the 7½% curve there is, in addition, a dip in effectiveness at M = 0.95 associated with shock-induced boundary-layer separation.

Planform B which is of the same aspect ratio and taper ratio as planform A but with some sweepback, shows a reduction in the sudden drop in effectiveness, resulting mainly from the lower effectiveness at subsonic speeds. The transformation from subsonic to supersonic conditions occurs more smoothly and begins at a somewhat higher Mach number. No dip in either the 6% or the 7½% curve is apparent. These characteristics are consistent with the known effects of sweeping the control hinge line.

On planform C, in spite of a high wing leading-edge sweepback, the control effectiveness behaviour is similar to that of planform A indicating the importance of trailing-edge sweepback in determining the control characteristics.

5.2 Effects of the control chord ratio

The rolling-effectiveness curves for the 6% wings with control-chord to wing-chord ratios of 0.1, 0.25 and 0.4 for each of the three planforms are presented in Fig.6. There are no major differences between the curves for any one planform, apart from the difference in overall level expected from the changes in control area. The characteristics associated with each planform can clearly be seen; the rapid drop from subsonic to supersonic levels for planforms A and C and the smoother changeover and higher Mach number at which the change occurs for planform B.

In terms of linearized theory the effectiveness at supersonic speeds should be directly proportional to the c_ξ/c ratio, so the effectiveness curves have been recomputed to show the variation of $\ell_\xi / c_\xi/c$ with Mach number. This parameter should collapse the data for supersonic speeds onto a single curve for each of the planforms if linearized theory is adequate. This has been done using values of ℓ_ξ, calculated as described in section 3, and the results in Fig.11 indeed show a reasonable collapse onto a single curve. This is only true at supersonic speeds when the control has little or no influence on the flow over the rest of the wing. At subsonic speeds the effectiveness conforms to no such pattern and $\ell_\xi / c_\xi/c$ has markedly different values for the three control-chord ratios tested. This is because in subsonic flow the presence of a control surface changes the flow over the rest of the wing, hence the smaller controls are more effective when compared on the basis of $\ell_\xi / c_\xi/c$.

5.3 Aileron-effectiveness derivative: ℓ_ξ

The aileron-effectiveness derivative ℓ_ξ has been calculated throughout the Mach number range for the three wings with t/c = 7½%, one of each

planform, from the measured rolling effectiveness and values of the damping in roll from Ref.1 (see Table 3 and Fig.8). The results for ℓ_ξ are plotted in Fig.9 and again the characteristics of the three planforms can be seen; the sudden drops in effectiveness at transonic speeds for planforms A and C and the relatively smooth curve for the swept-back planform B. Outside the transonic speed range the curves follow very similar trends with Mach number.

The derivative ℓ_ξ has been calculated for the various wings with t/c = 0.06 and plotted in Figs.10a-d. The values of ℓ_p used in the calculations were those measured on the 7½% t/c wings apart from the transonic region (M = 0.9 to 1.1) on planforms A and B where a linear variation between the subsonic and supersonic levels was assumed. For planform C only the subsonic and supersonic values of ℓ_ξ are presented since the ℓ_p measurements on this planform show evidence of marked thickness effects.

5.4 Results from the models with tip controls Nos. 13, 14, 15 and 16

The rolling effectiveness curves of $\bar{p}b/2V\xi$ for the tip-control models are plotted in Fig.7. The planform characteristics noted on all flap-control models are now absent, apart from the curve for model 16, which shows the original planform C characteristic of a sudden drop in effectiveness transonically. Models 13, 14 and 15 of planforms A, B and C respectively had streamwise hinge lines with the hinge point at the mid-chord position and each showed a smooth transformation across the transonic speed range, with a small rise in effectiveness for planform A, compared with the sudden drop associated with the flap-controls.

Model 16 had a hinge line inclined at 50° to the trailing edge and was hinged at one third of the chord back from the leading edge. This configuration behaved more like the flap-control models and had the usual transonic drop in effectiveness. This again emphasises the importance of the sweepback of the hinge line in determining the behaviour. It should be noted that the gap between the wing and the control was not faired in and may well be acting as a leading edge notch and thus be stabilizing separations in the flow. The aileron effectiveness, ℓ_ξ, has been computed for these tip-control models in a similar way to the other wings with t/c = 0.06 and the results plotted in Fig.10d.

6 CONCLUSIONS

1 At supersonic speeds measurements of the rolling-effectiveness derivative ℓ_ξ on a number of wings with flap controls confirm linearized supersonic theory in that for a given wing planform and control span the control effectiveness is proportional to control area.

2 At transonic speeds the wings with flap controls showed the drop in control effectiveness characteristic of such layouts with additional dips attributed to shock/boundary layer effects on the thicker wings. Adverse thickness effects were removed by increase in the sweepback of the control hinge line.

3 The wings fitted with all-moving-tip controls showed no evidence of marked changes in control effectiveness at transonic speeds.

LIST OF SYMBOLS

b diameter of the circle which circumscribes the wing tips, ft

c wing chord

c_ξ control chord

L_ξ aileron-effectiveness derivative: rate of change of rolling moment with aileron-deflexion angle

L_p roll-damping derivative: rate of change of rolling moment with rate of roll

ℓ_ξ non-dimensional aileron-effectiveness derivative $= \dfrac{L_\xi}{\rho V^2 S \frac{b}{2}}$

ℓ_p non dimensional roll-damping derivative $= \dfrac{L_p}{\rho V S \left(\frac{b}{2}\right)^2}$

M Mach number

$\bar{p}$ rate of roll, the bar denotes under steady conditions; degrees/sec

S reference area, sq ft. Here taken as 3/2 times the gross wing area of a pair of wing panels

t wing thickness

V velocity, ft/sec

ξ control-deflexion angle, degrees

ρ atmospheric density, slugs/cu ft

LIST OF REFERENCES

No.	Author(s)	Title, etc.
1	Turner, K.J. Hunt, G.K.	Free-flight measurements of the transonic roll-damping characteristics of three related wings of aspect ratio 2.83. A.R.C. 22,117. April, 1960.
2	Lawrence, T.F.C. Swan, J.	Development of a transonic research technique using ground-launched rocket-boosted models. Part 1. Control effectiveness measurements. A.R.C. 13,740. July, 1950.
3	Broadbent, E.G.	The rolling power of an elastic swept wing. A.R.C. R. & M. 2857. July, 1950.

TABLE 1

Details of the models

Model number	Type of planform	Wing details		Control details			Method of construction See Table 2	$\frac{\bar{pb}}{2V\xi}$ results shown in Fig. No.	Control type
		Thickness: chord ratio		Chord ratio $\frac{c_\xi}{c}$	Deflexion ξ, degrees	Trailing edge angle ε, degrees			
1	A	6%	Section R.A.E. 102 Aspect ratio 2.83 Taper ratio 0.333 Leading edge sweepback 28°	0.25	5° 2'	6.5	2	5 & 6	OUTBOARD HALF SPAN
2		7½%		0.25	5° 20'	8.2	1	5	
3		6%		0.40	5° 5'	6.5	2	6	
4		6%		0.10	9° 37'	6.5	3	6	
5	B	6%	Section R.A.E. 102 Aspect ratio 2.83 Taper ratio 0.333 Leading edge sweepback 53° 30'	0.25	4° 59'	6.5	1a	5 & 6	
6		7½%		0.25	4° 48'	8.2	1	5	
7		6%		0.40	5° 12'	6.5	1	6	
8		6%		0.10	9° 26'	6.5	3	6	
9	C	6%	Section R.A.E. 102 Aspect ratio 2.83 Taper ratio 0.086 Leading edge sweepback 50°	0.25	4° 55'	6.5	2	5 & 6	
10		7½%		0.25	4° 52'	8.2	2	5	
11		6%		0.40	4° 58'	6.5	2	6	
12		6%		0.10	9° 56'	6.5	3a	6	
13	A	6%	See above and also Fig.1 for control details	Span ratio 25%	5° 4'	6.5	1	7	Tip controls
14	B	6%		25%	5° 1'	6.5	1	7	
15	C	6%		25%	4° 45'	6.5	1	7	
16	C	6%		25%	4° 56'	6.5	1	7	

TABLE 2

Methods of model wing and control construction

Each model listed in Table 1 has a method-of-construction number associated with it. Below are listed the main features of each method

Number	Method of construction
1	Each wing is made of a core of light-alloy plates glued together which roughly form the wing section and planform. The core is then covered with laminations of compressed wood and shaped to the correct section required. This is done to ensure ease of manufacture, together with reasonable stiffness properties. The core does not extend to the trailing edge, which is made from Tufnol to avoid the warping that was found on a compressed-wood trailing edge. The controls are made from compressed wood and Tufnol edges with no core and are pinned and glued at the required setting angle.
1a	As in type 1 above but with compressed wood trailing edges instead of Tufnol.
2	The wings are as in type 1 above. The controls are machined from light alloy and attached as above.
3	The wings again had a light-alloy core with compressed-wood laminations as the surface but the core extends through to the trailing edge. The core is machined to form the inboard part of the trailing edge and the control surfaces all in one. The control part is then bent to the desired angle whilst remaining an integral part of the wing core.
3a	As in type 3 above but the alloy core is surfaced with Araldite instead of compressed wood.

TABLE 3

Values of damping-in-roll derivative $-\ell_p$ from Ref.1

(These are plotted in Fig.8)

Mach Number	Planform A $-\ell_p$	Planform B $-\ell_p$	Planform C $-\ell_p$
0.8	0.250	0.200	0.255
0.82	0.255	0.210	0.257
0.84	0.260	0.220	0.260
0.86	0.261	0.225	0.263
0.88	0.263	0.230	0.268
0.90	0.263	0.233	0.273
0.92	0.260	0.231	0.280
0.94	0.266	0.232	0.291
0.96	0.330	0.248	0.225
0.98	0.353	0.250	0.180
1.00	0.353	0.267	0.264
1.02	0.353	0.285	0.269
1.04	0.352	0.300	0.265
1.06	0.352	0.305	0.262
1.08	0.356	0.305	0.260
1.10	0.360	0.307	0.257
1.12	0.361	0.309	0.255
1.14	0.363	0.307	0.254
1.16	0.365	0.305	0.254
1.18	0.366	0.300	0.254
1.20	0.370	0.297	0.255
1.22	0.375	0.295	0.256
1.24	0.385	0.290	0.258
1.26	0.390	0.287	0.259
1.28	0.387	0.283	0.259
1.30	0.380	0.281	0.258
1.32	0.363	0.277	0.256
1.34	0.363	0.273	0.254
1.36	0.363	0.271	0.252
1.38	0.363	0.270	0.250
1.40	0.363	0.269	0.248

WT.2078.C.P.572.K3 - Printed in England

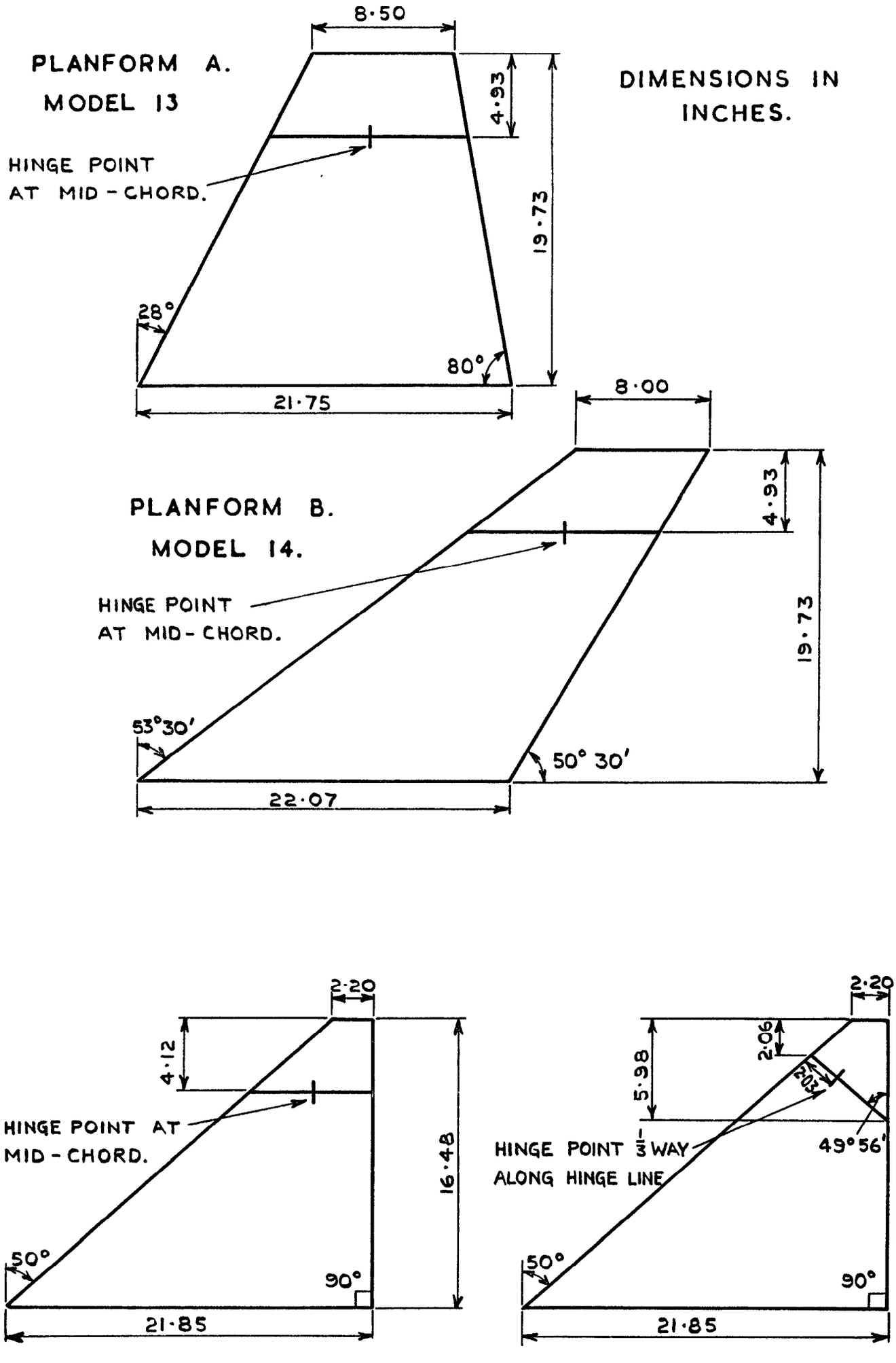

FIG. 1. MODEL PLANFORMS SHOWING. TIP CONTROLS.

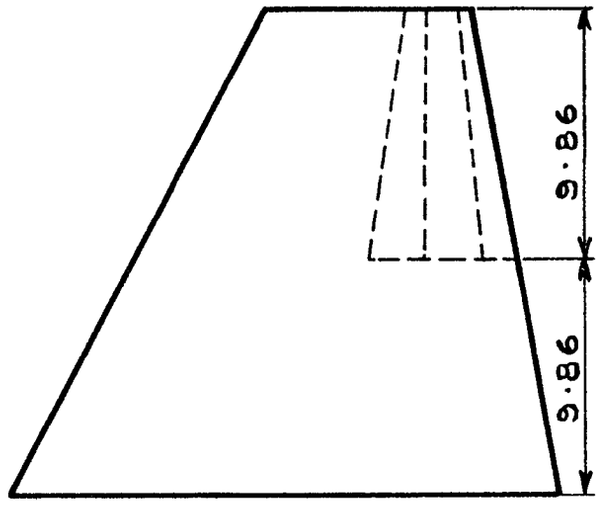

DIMENSIONS IN INCHES.

PLANFORM A.
MODELS 1,2,3,4 & 5.

PLANFORM B.
MODELS 6,7,8,9 & 10

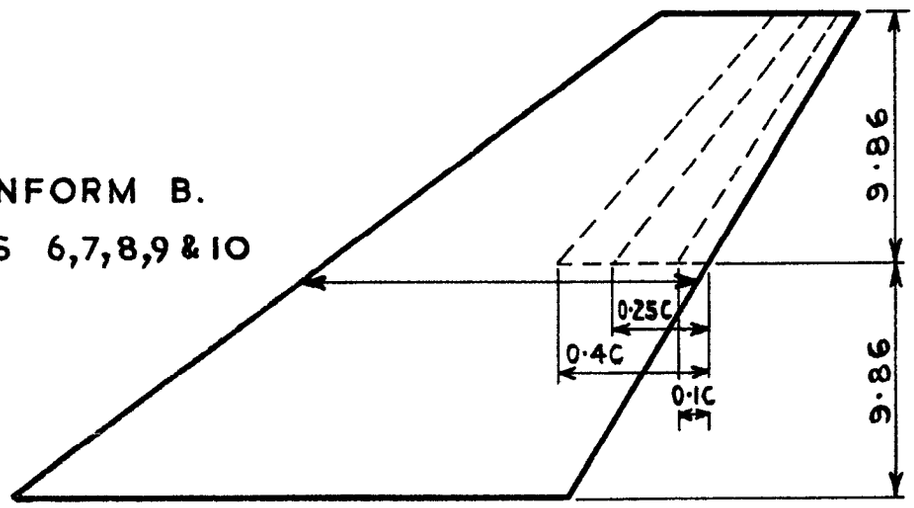

THE CONTROL POSITIONS SHOWN ARE ALL $C_f/C = 0.1$, $C_f/C = 0.25$ AND $C_f/C = 0.4$ AND EXTEND OVER THE OUTBOARD HALF-SPAN.

PLANFORM C.
MODELS 11,12,13,14 & 15

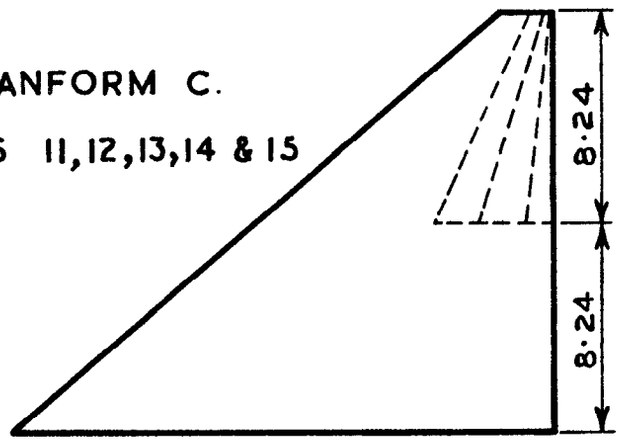

FIG. 2. MODEL PLANFORMS SHOWING FLAP-CONTROL POSITIONS.

a. PLANFORM A. MODEL No.4

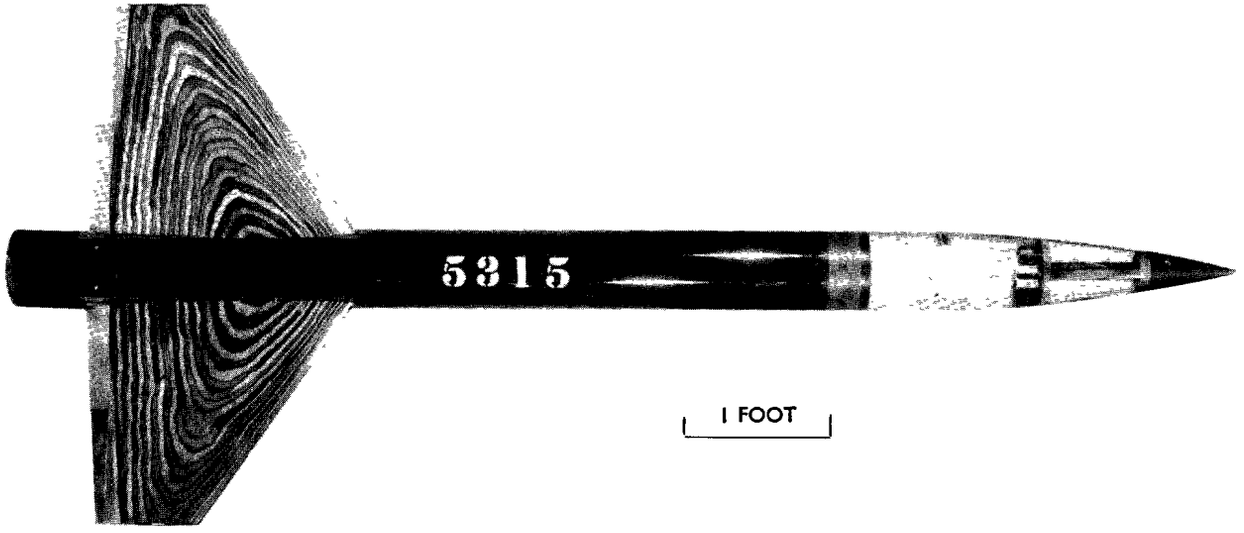

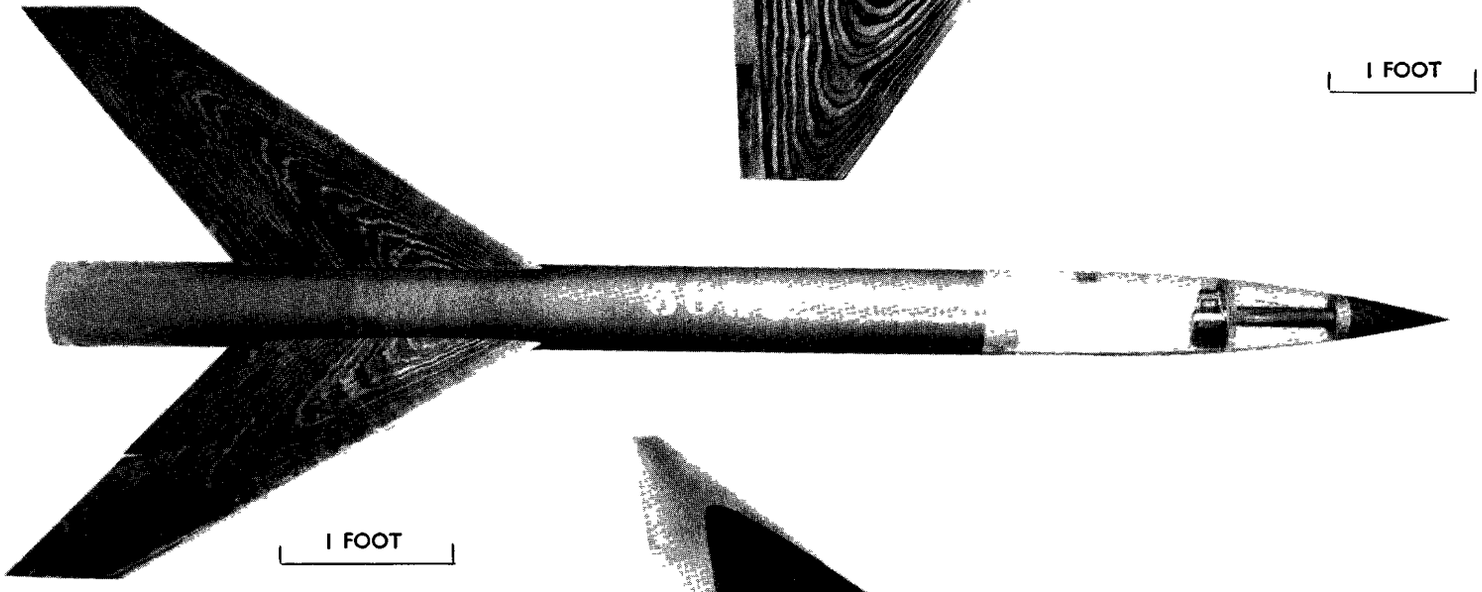

b. PLANFORM B. MODEL No.5

c. PLANFORM C. MODEL No.12

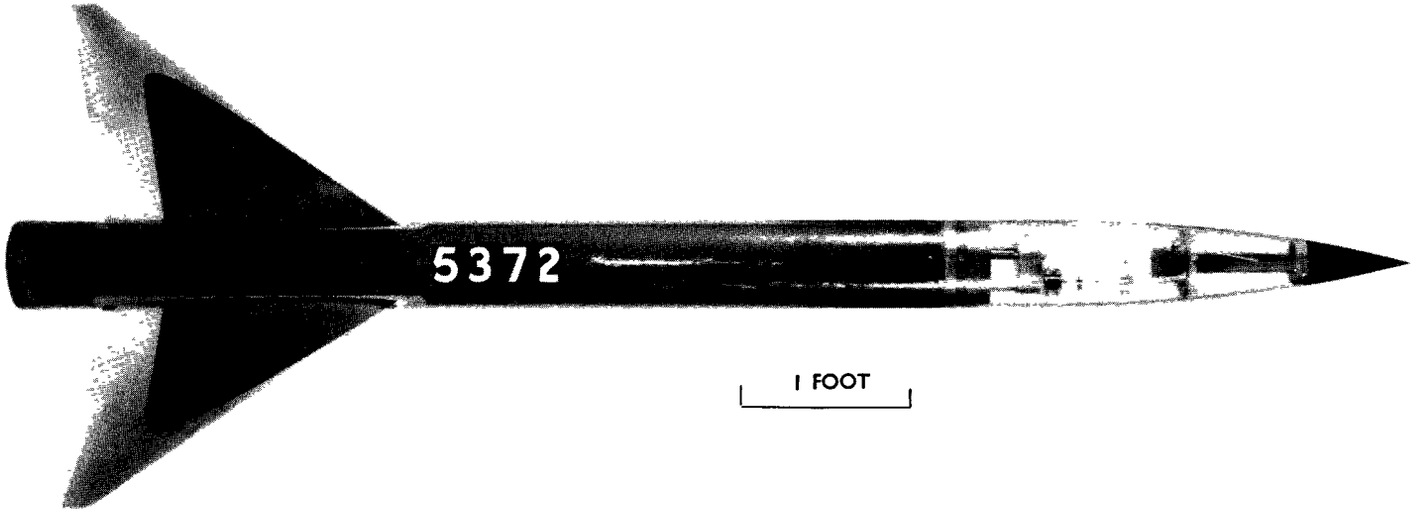

FIG.3. TEST VEHICLES

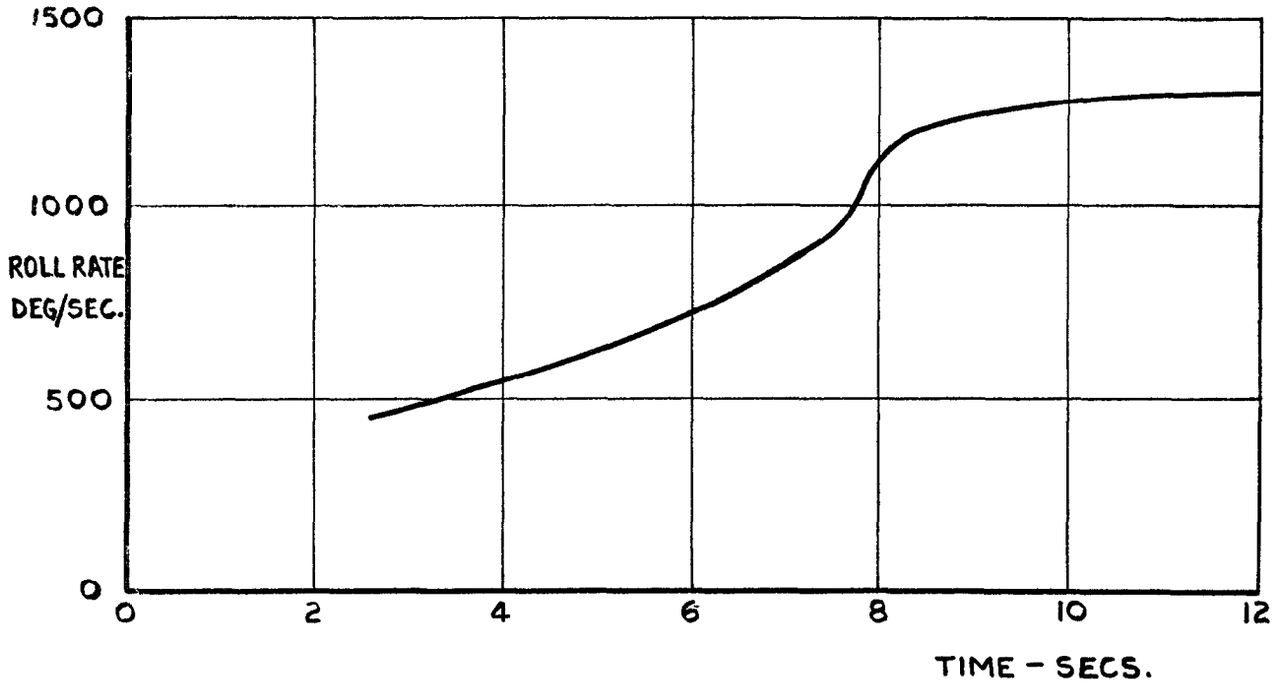

(a). RATE OF ROLL.

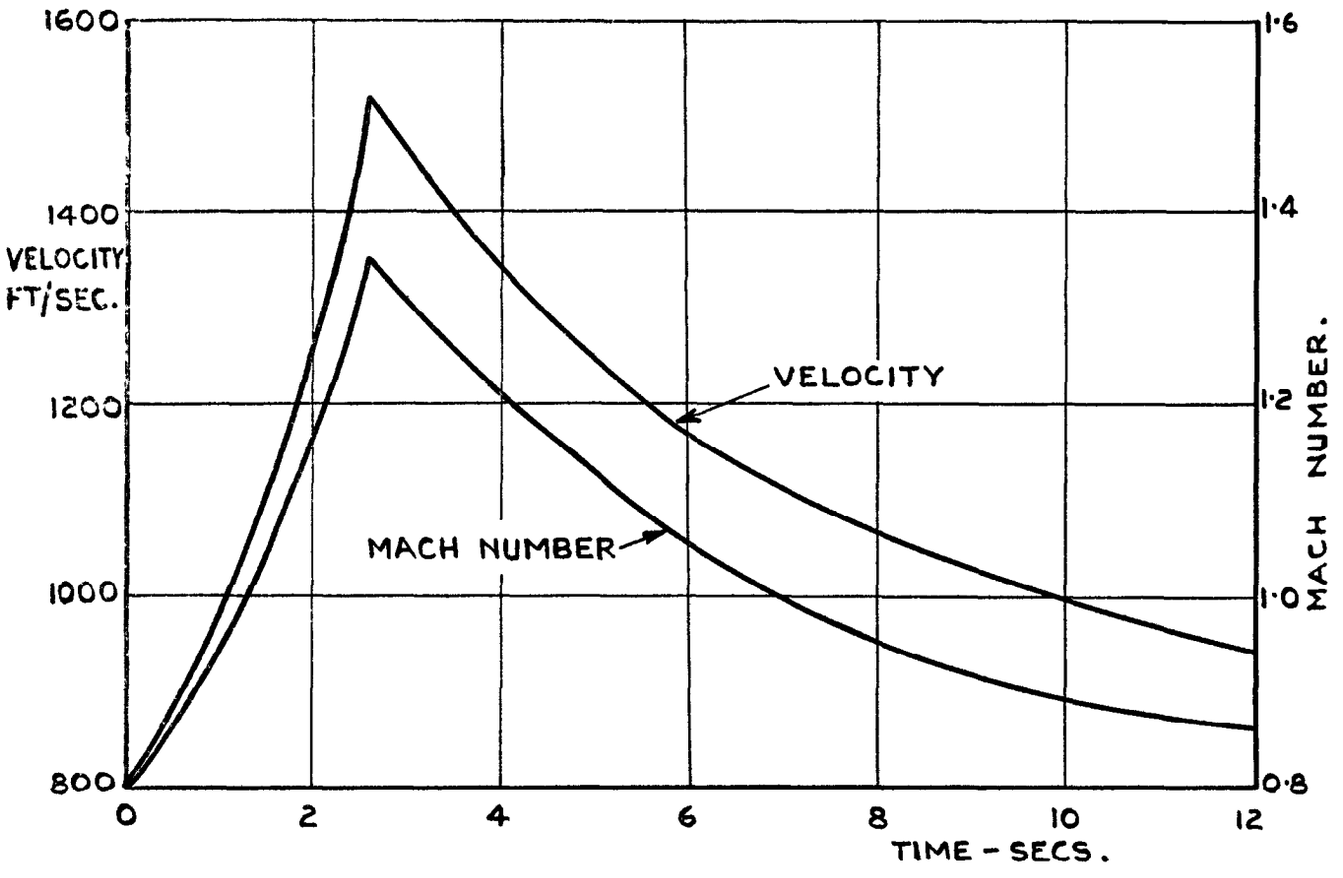

(b) VELOCITY AND MACH NUMBER.

FIG. 4 (a&b) TYPICAL VEHICLE PERFORMANCE.
(MODEL 8)

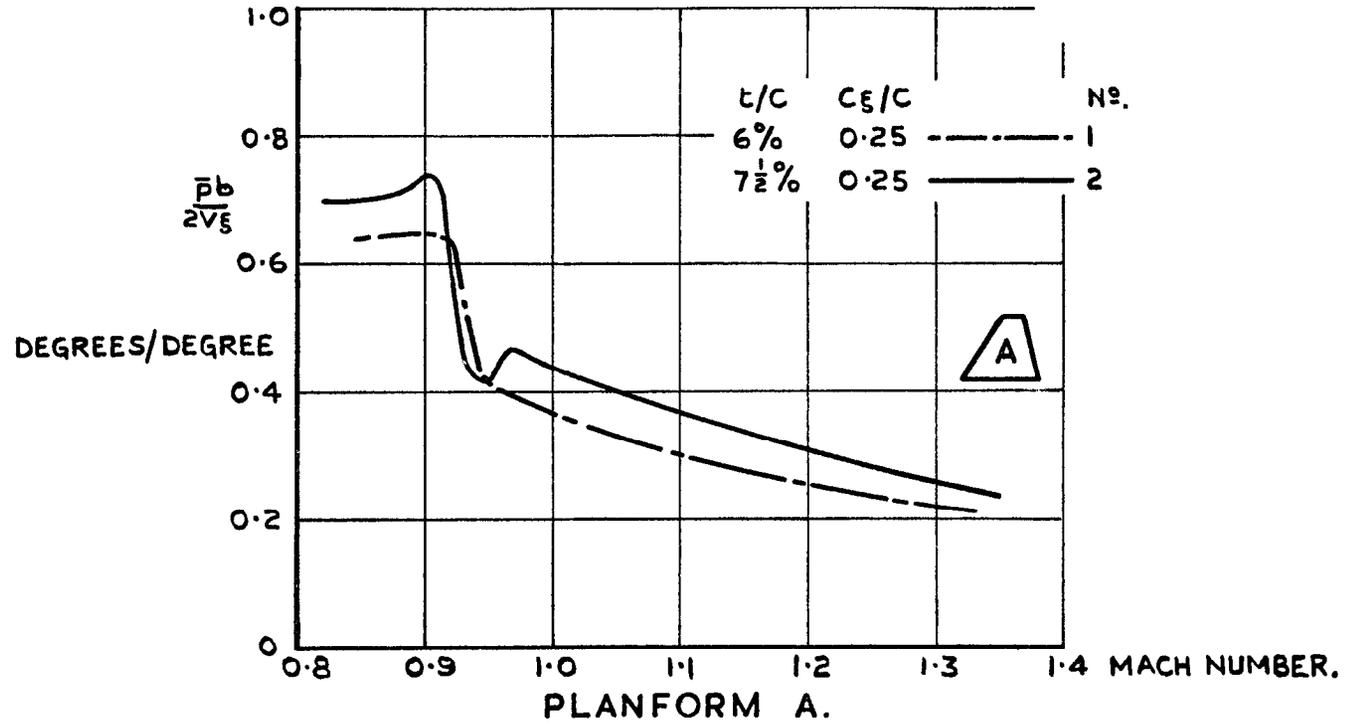

PLANFORM A.

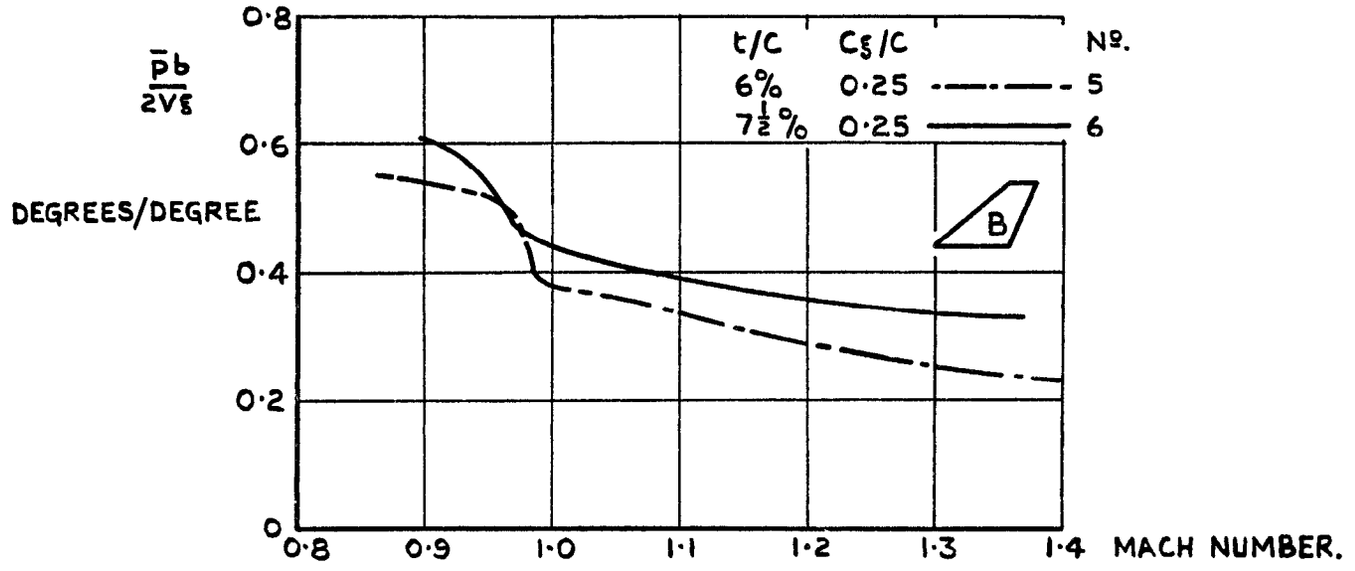

PLANFORM B.

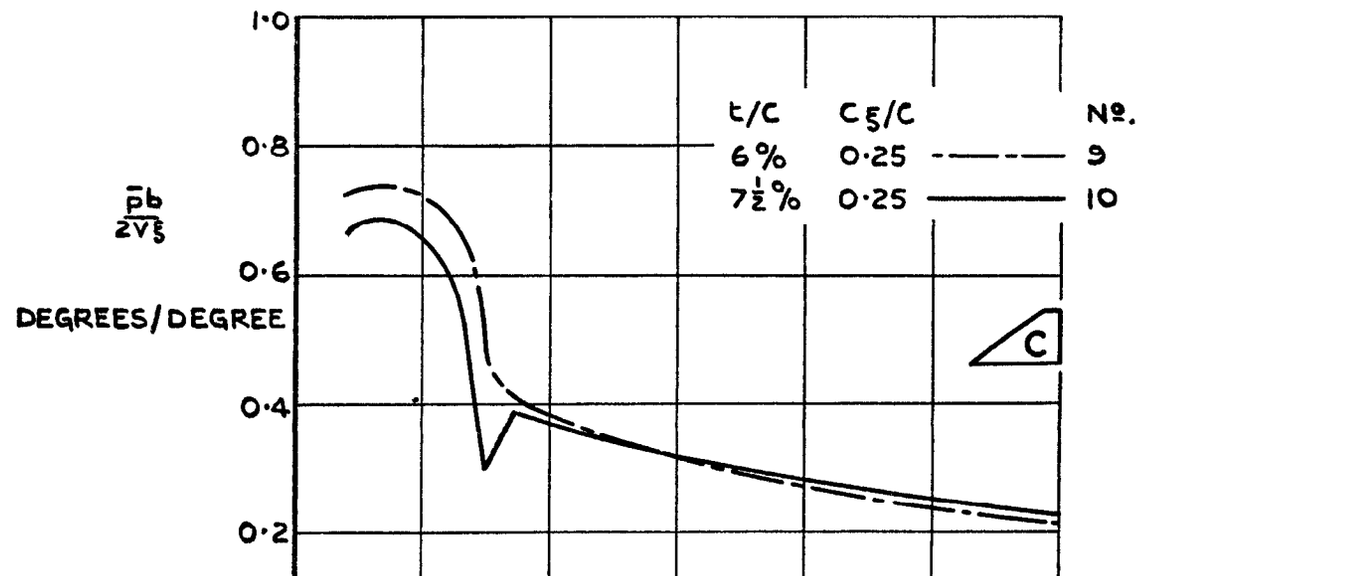

PLANFORM C.

FIG. 5. ROLLING EFFECTIVENESS. VARIATION WITH THICKNESS/CHORD RATIO.

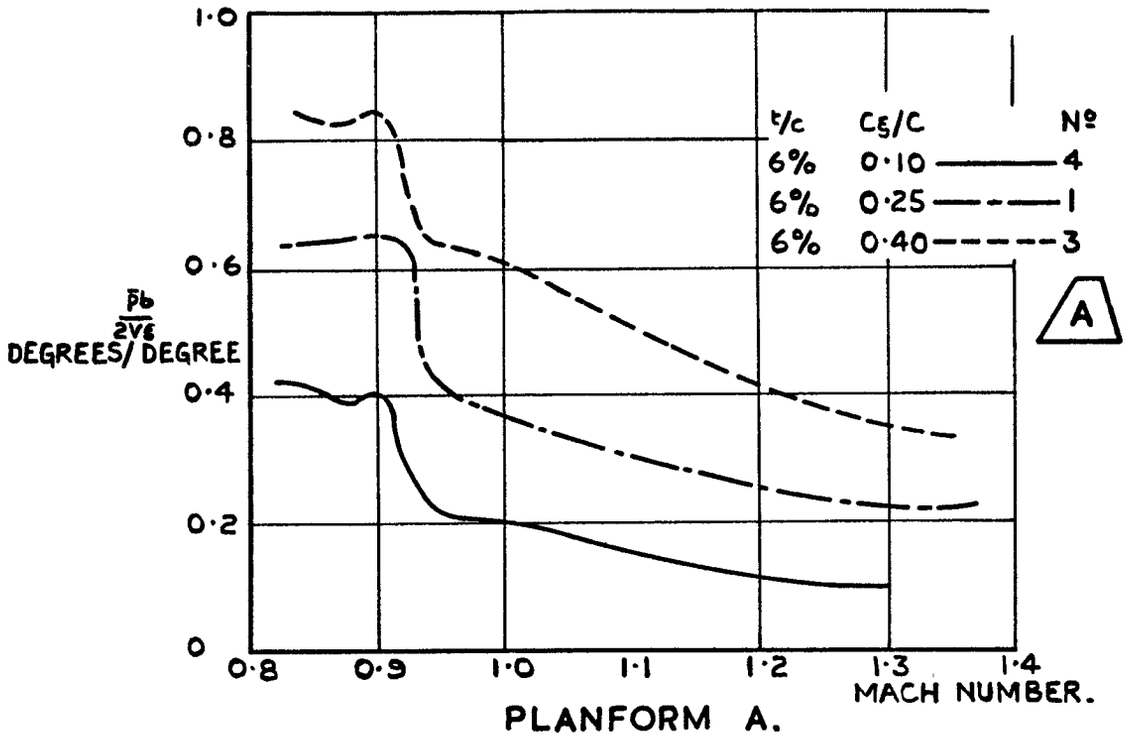

PLANFORM A.

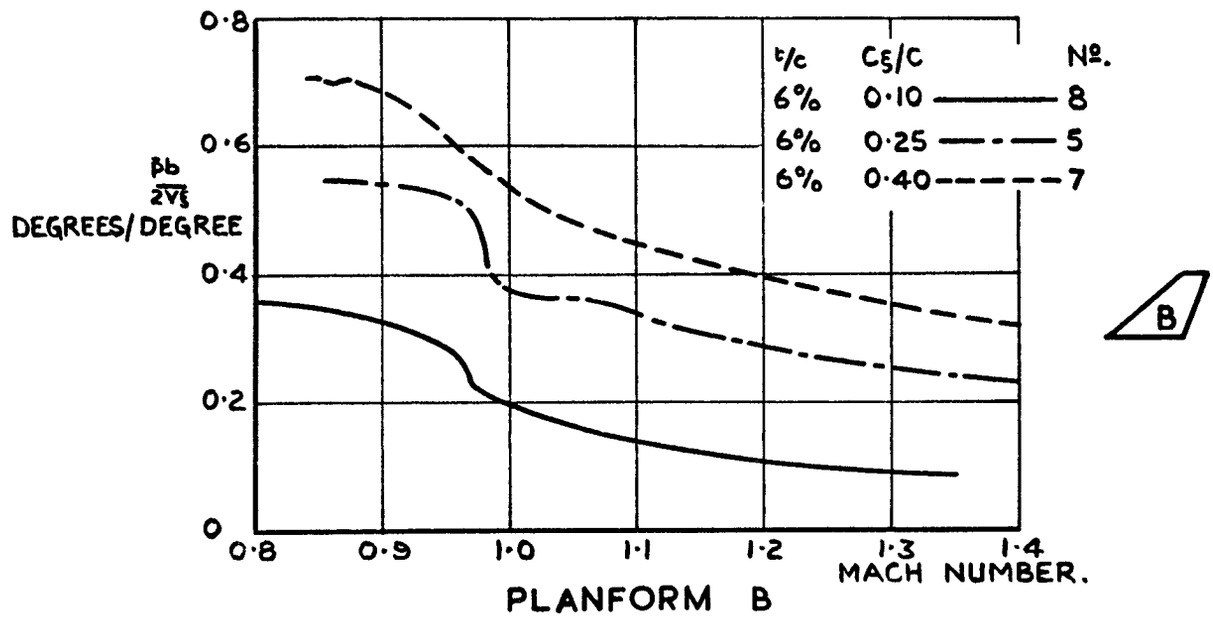

PLANFORM B

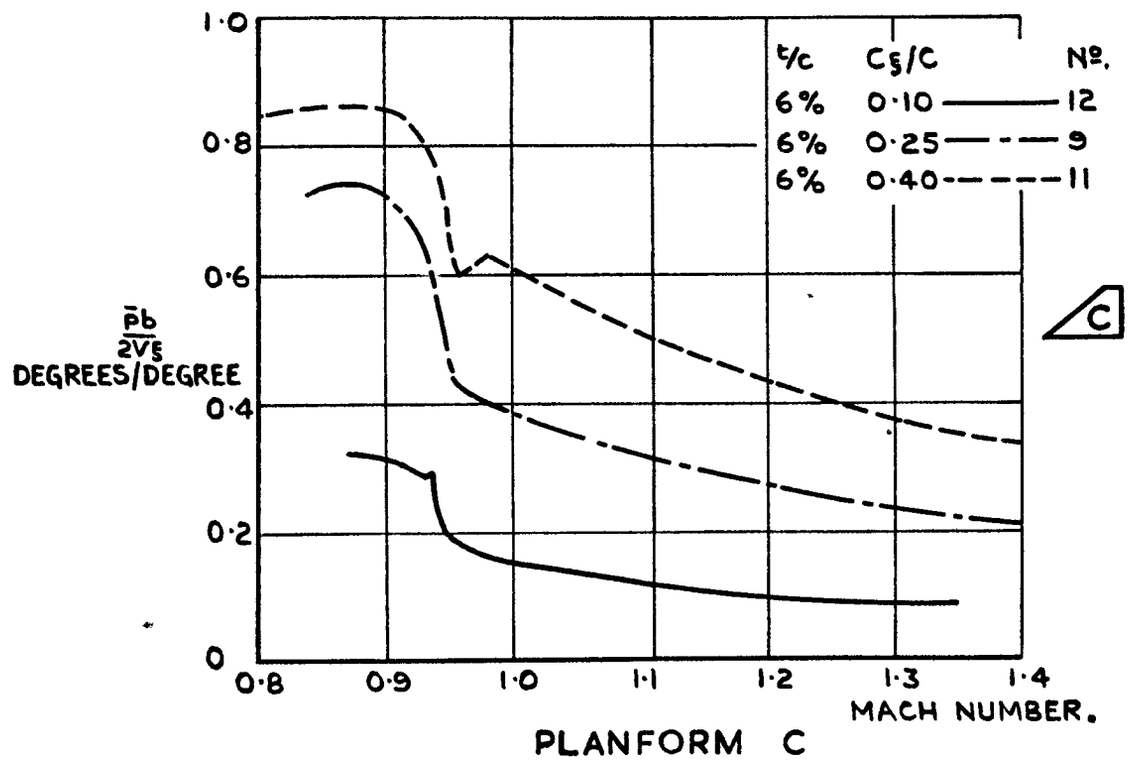

PLANFORM C

FIG. 6. ROLLING EFFECTIVENESS. VARIATION WITH CONTROL CHORD.

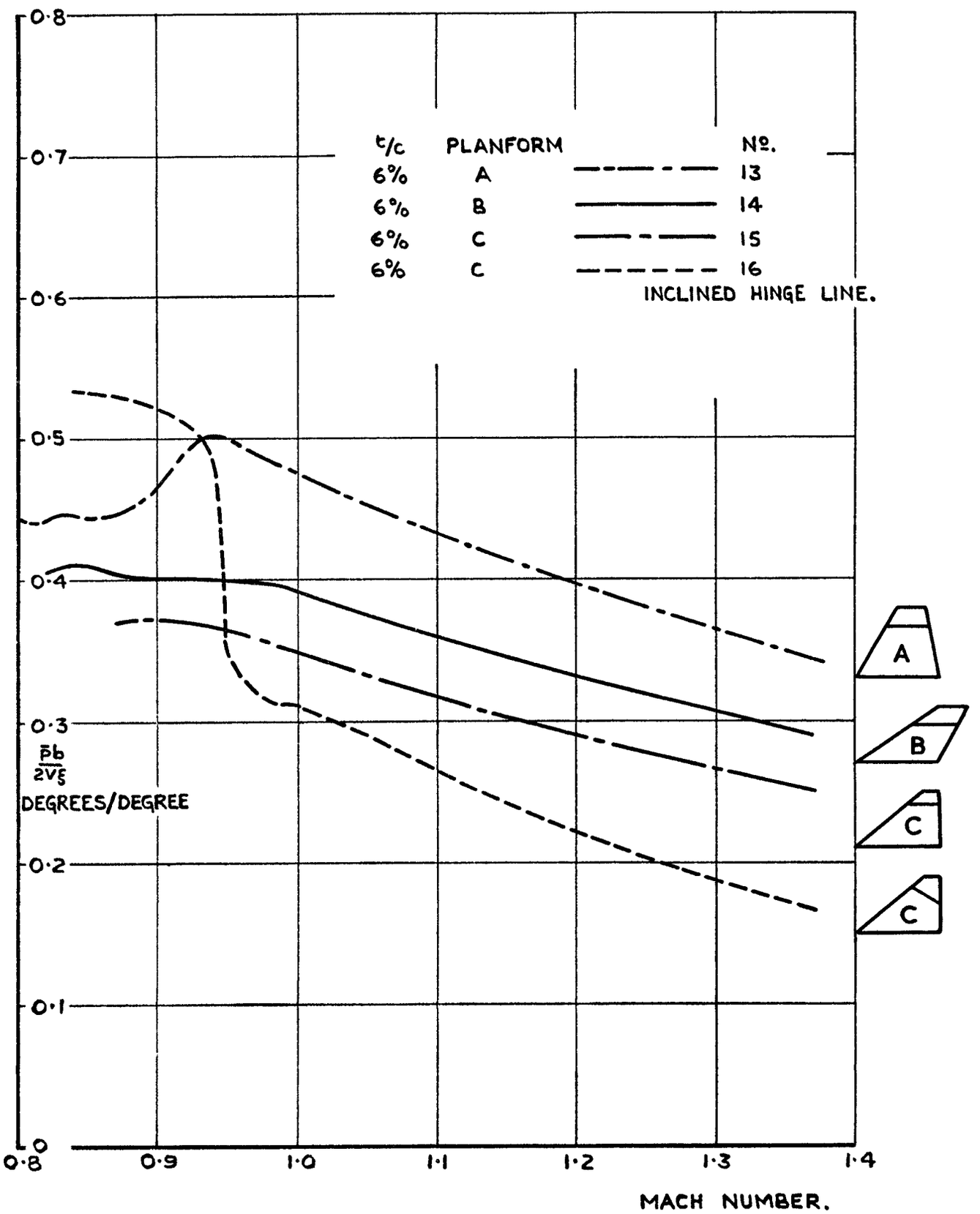

FIG. 7. ROLLING EFFECTIVENESS ALL-MOVING-TIP CONTROL VEHICLES.

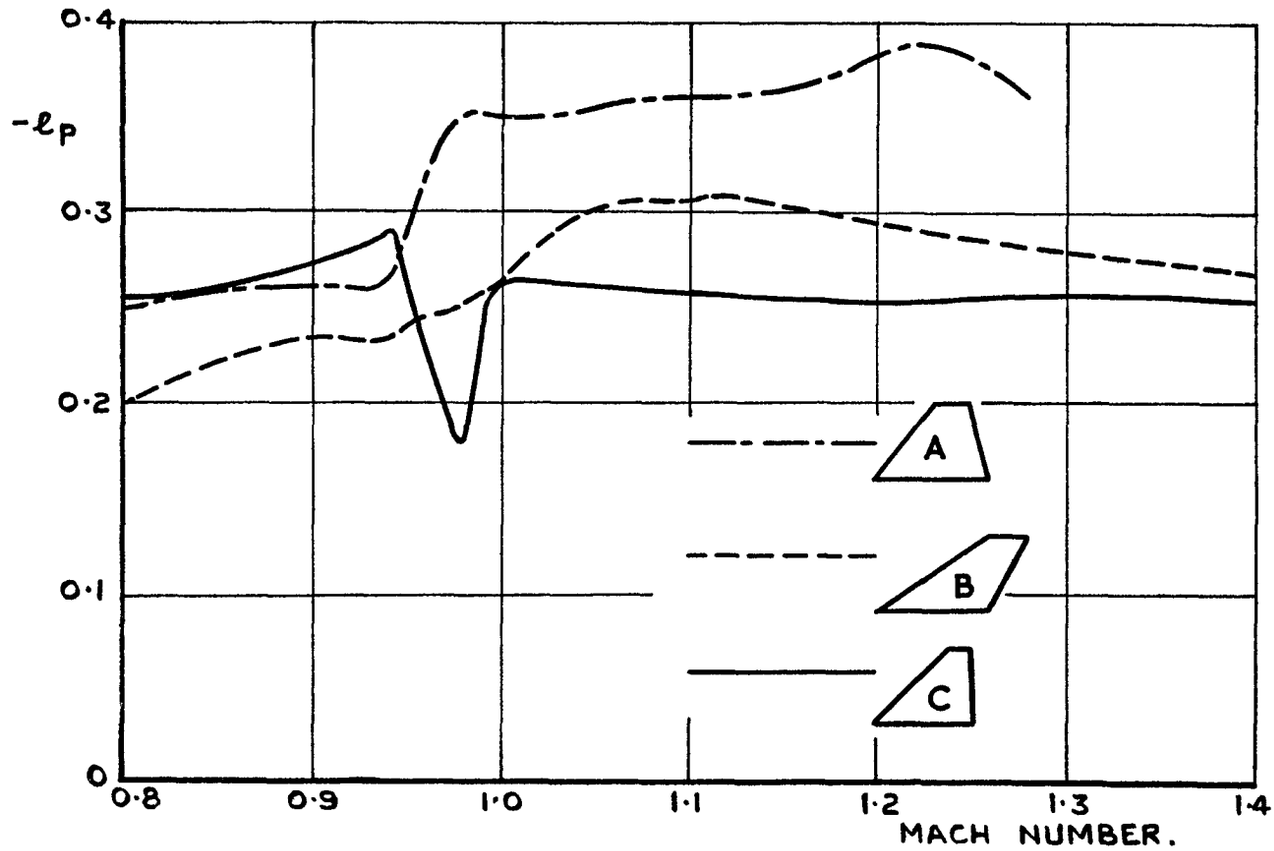

FIG. 8. ROLL-DAMPING DERIVATIVE ℓ_p. (FROM REF. 1).

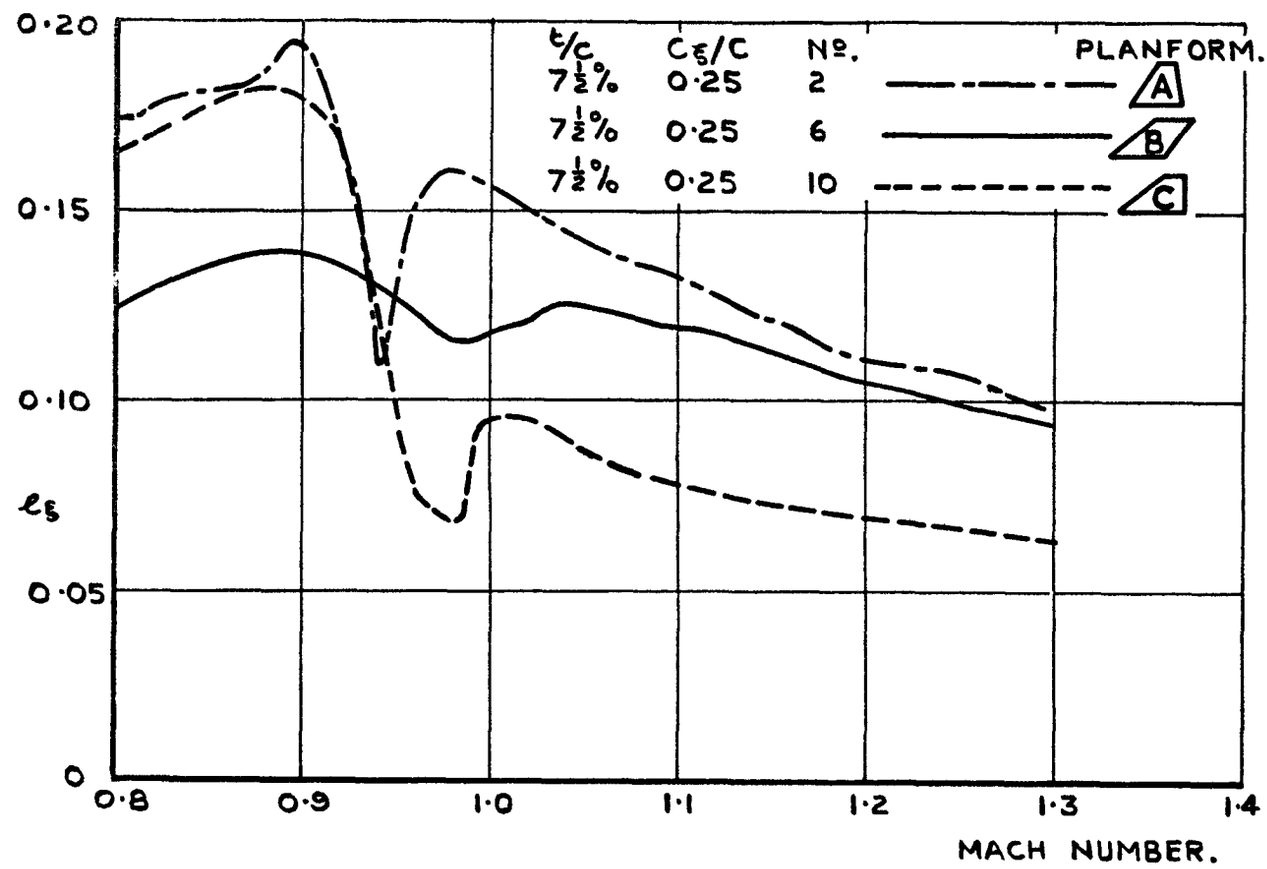

FIG. 9. AILERON EFFECTIVENESS DERIVATIVE ℓ_ξ FOR 7½ % t/c WINGS.

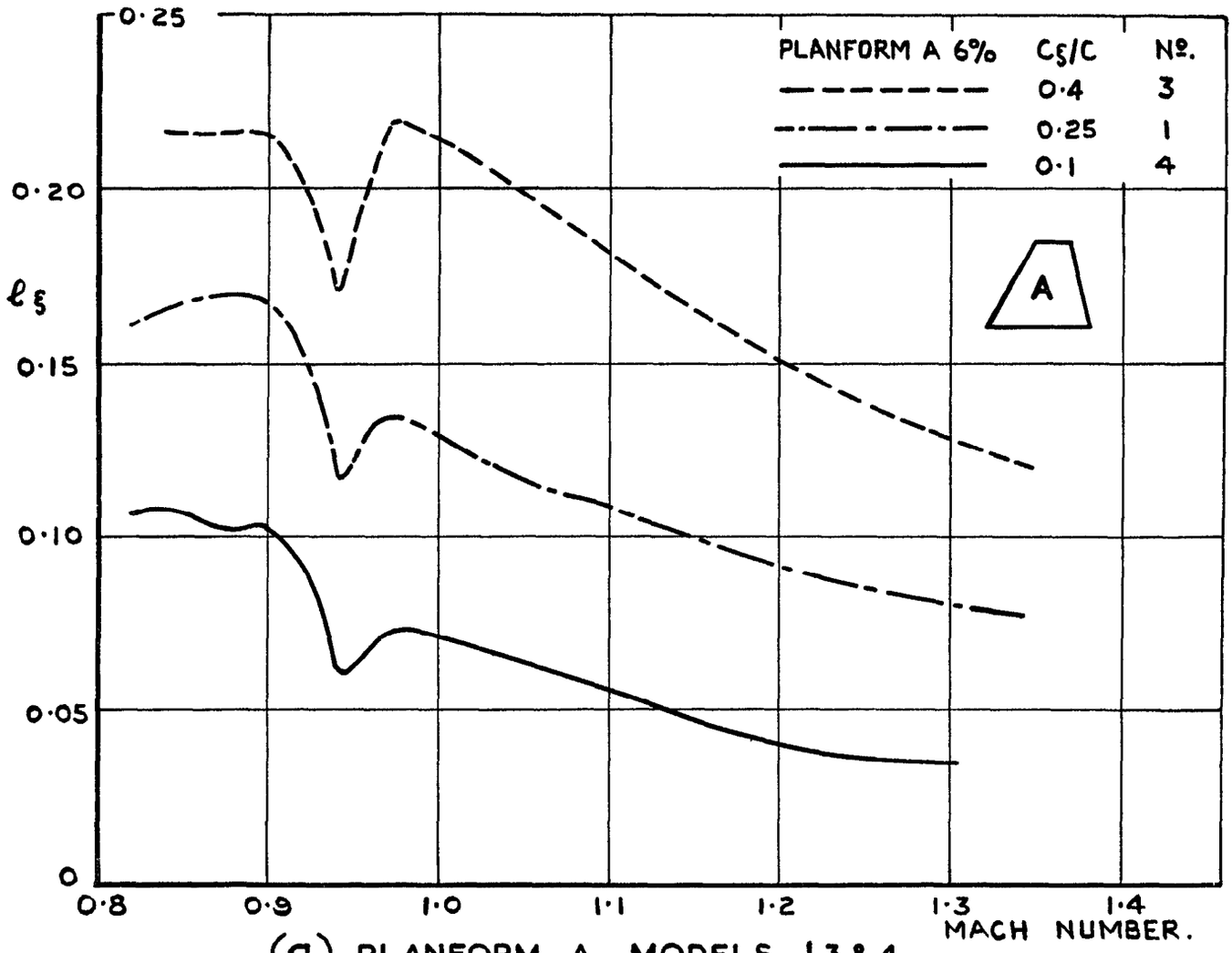

(a). PLANFORM A MODELS 1,3 & 4.

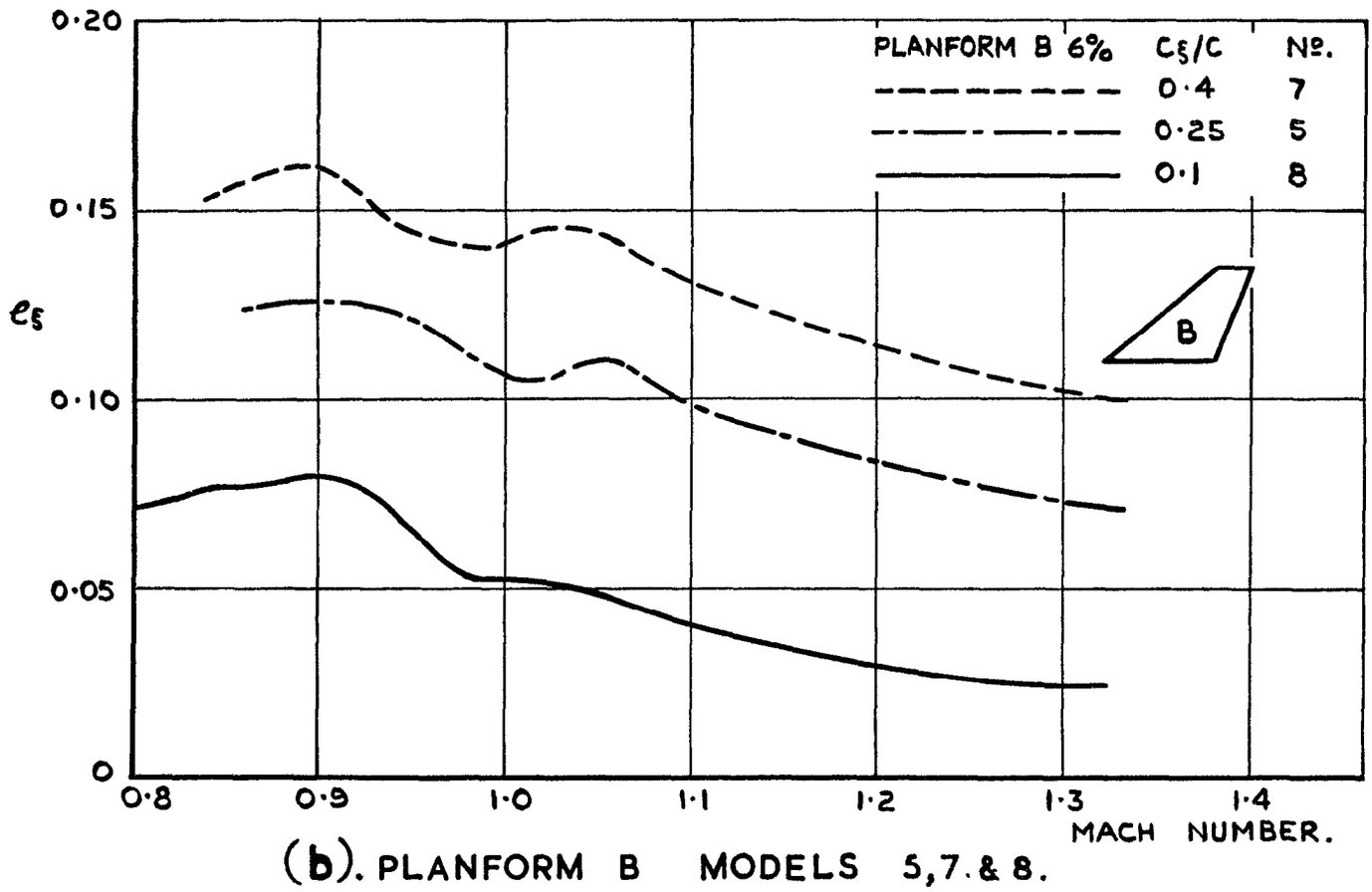

(b). PLANFORM B MODELS 5,7. & 8.

FIG. 10 (a & b). AILERON-EFFECTIVENESS DERIVATIVE ℓ_ξ FOR 6% $^t/_c$ WINGS OF PLANFORMS A&B.

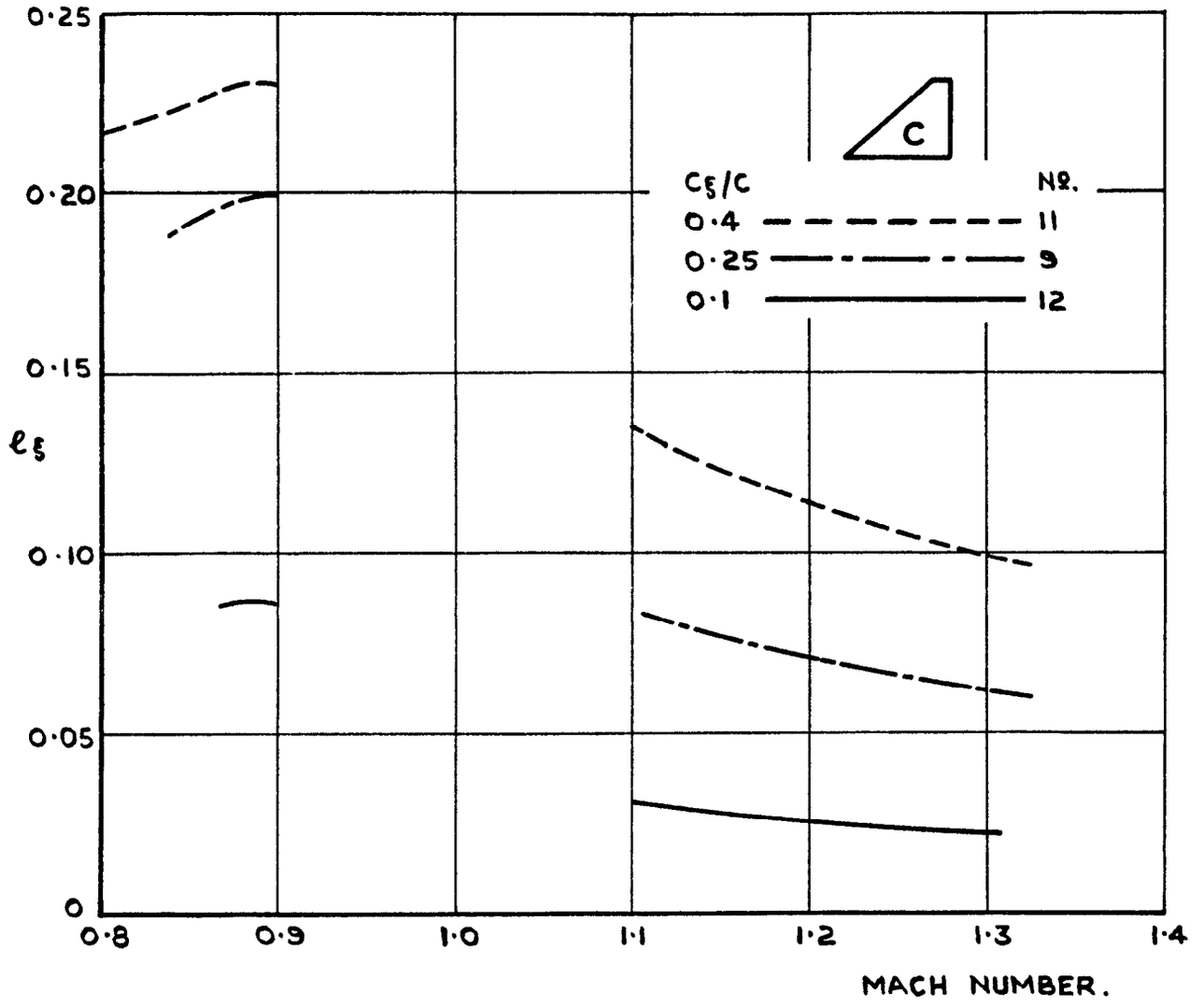

PLANFORM C Nº. 9 11 & 12 $t/c = 6\%$.

FIG. 10 (c). AILERON EFFECTIVENESS DERIVATIVE ℓ_ξ 6% t/c WING PLANFORM C.

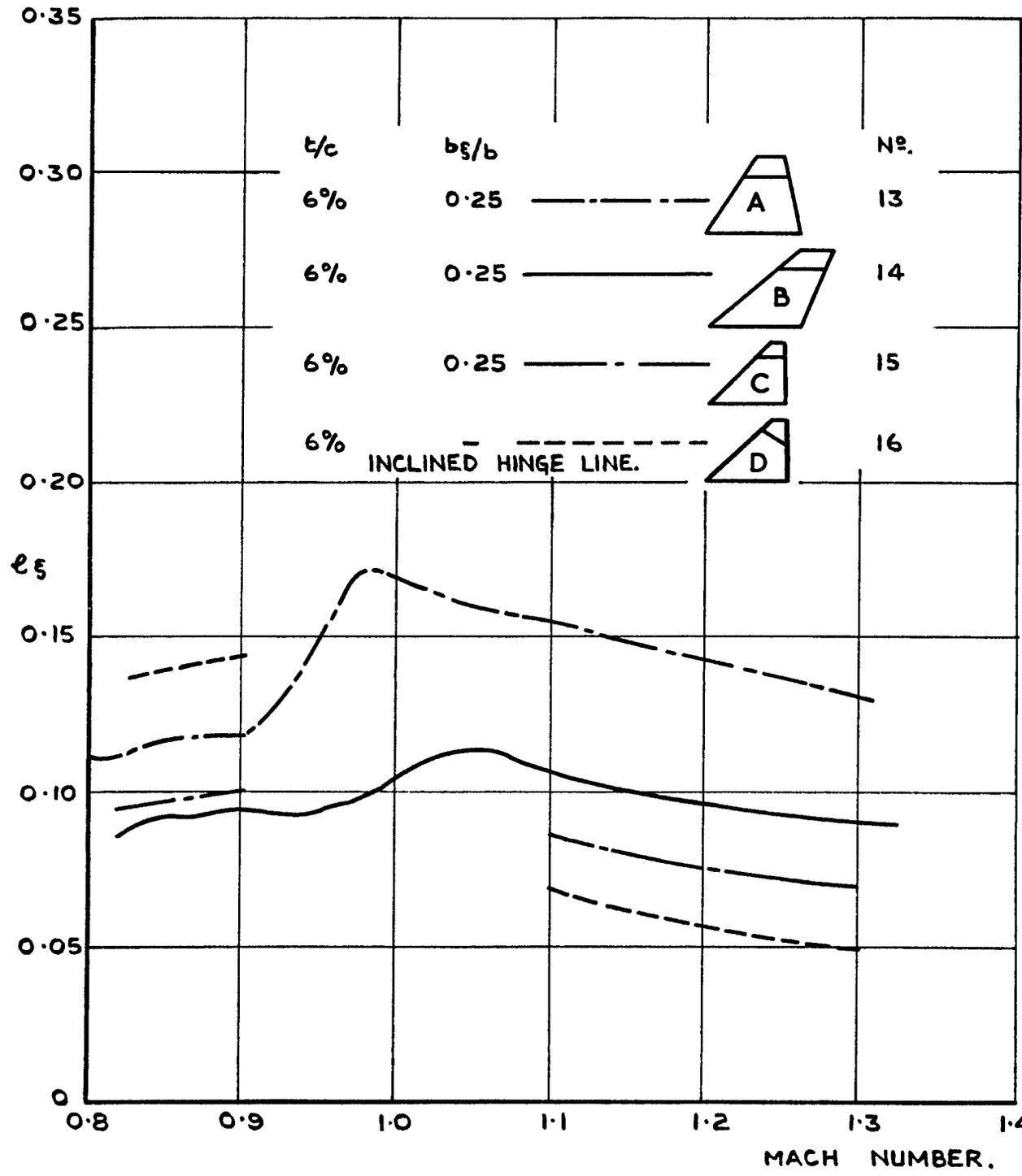

FIG. 10(d). AILERON EFFECTIVENESS DERIVATIVE ℓ_ξ 6% t/c WINGS WITH ALL-MOVING-TIP CONTROLS.

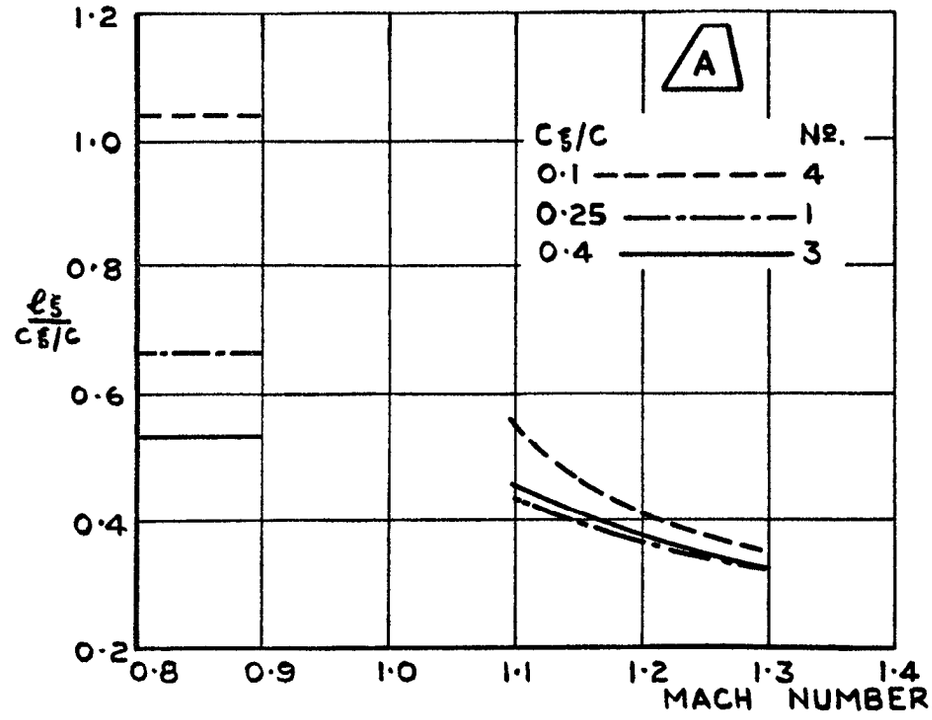

PLANFORM A.

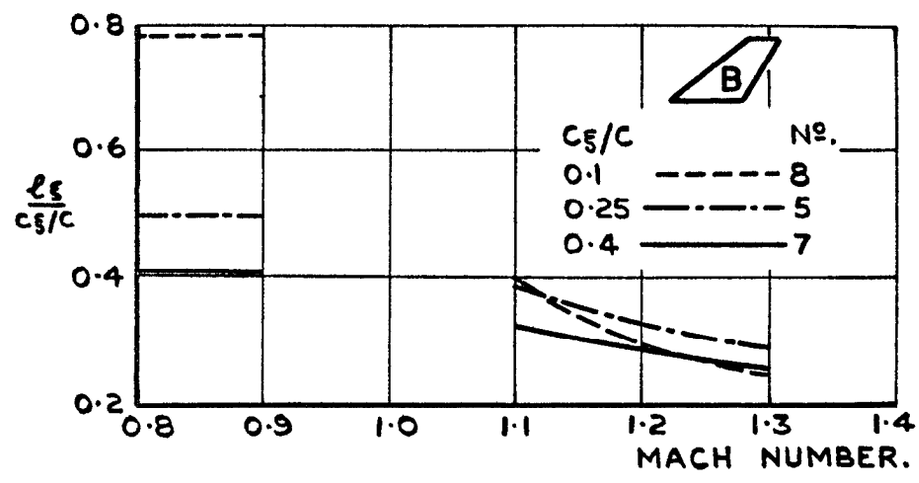

PLANFORM B.

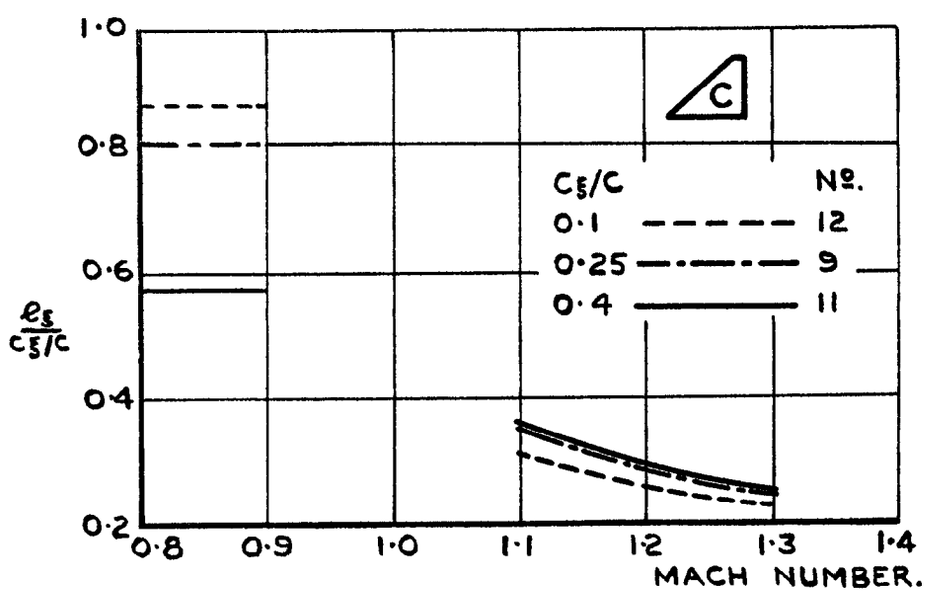

PLANFORM C.

FIG. 11. VARIATION OF $\frac{l_\xi}{c_{\xi/C}}$ WITH MACH NUMBER PLANFORMS A,B & C

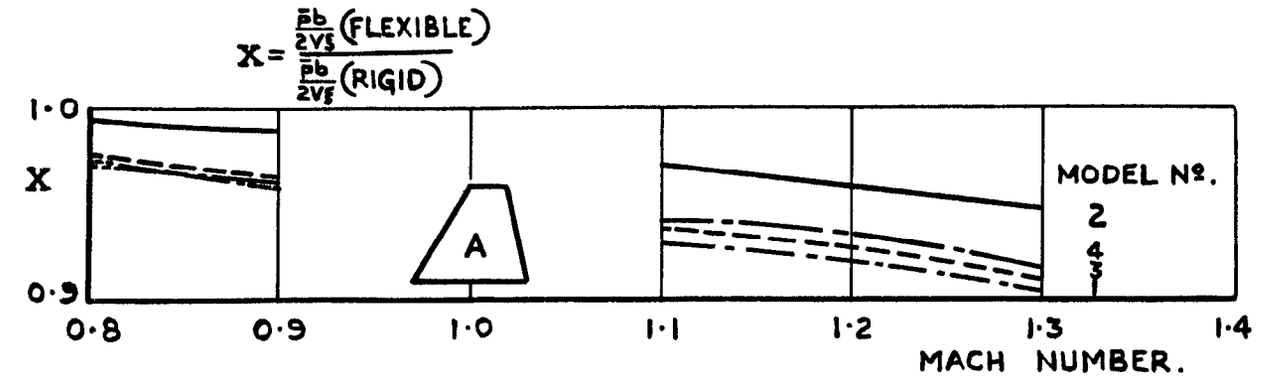

PLANFORM A.

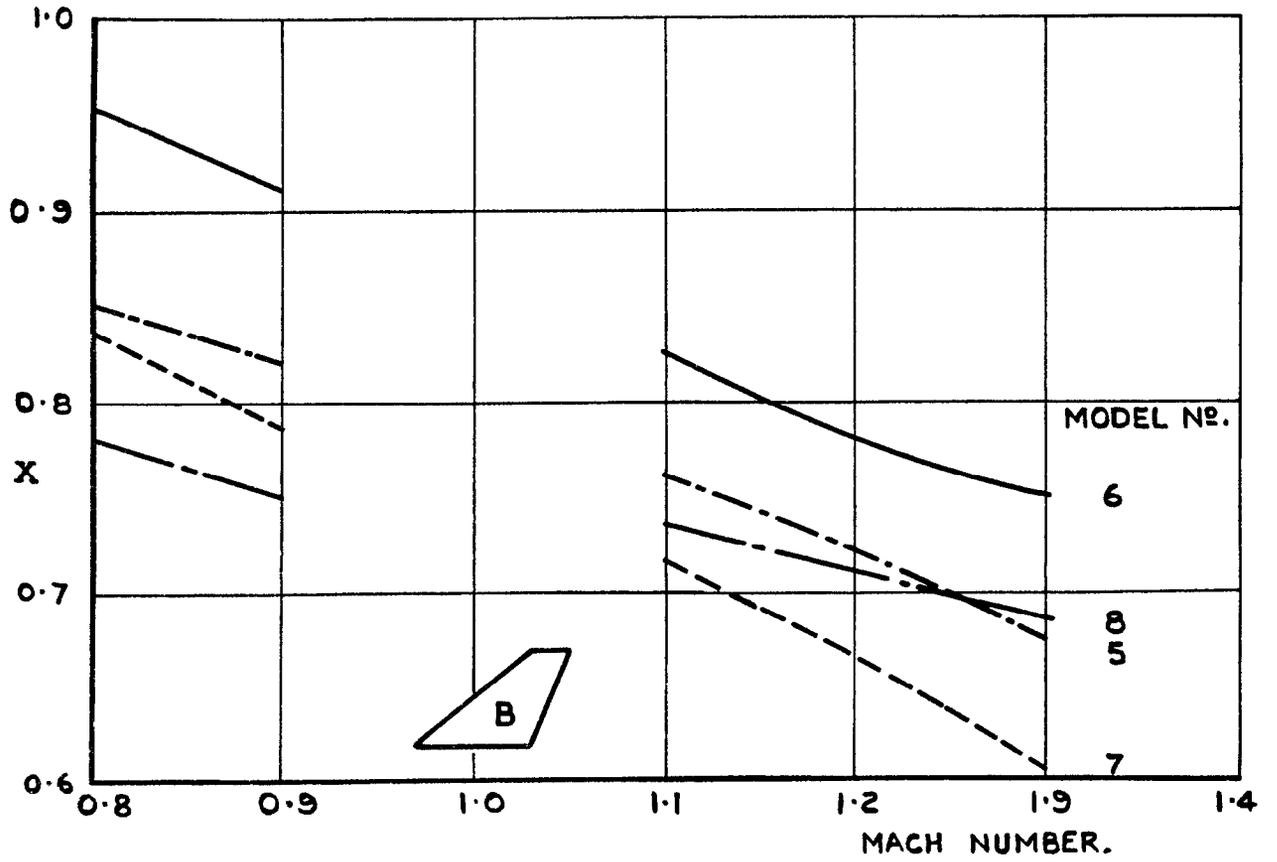

PLANFORM B

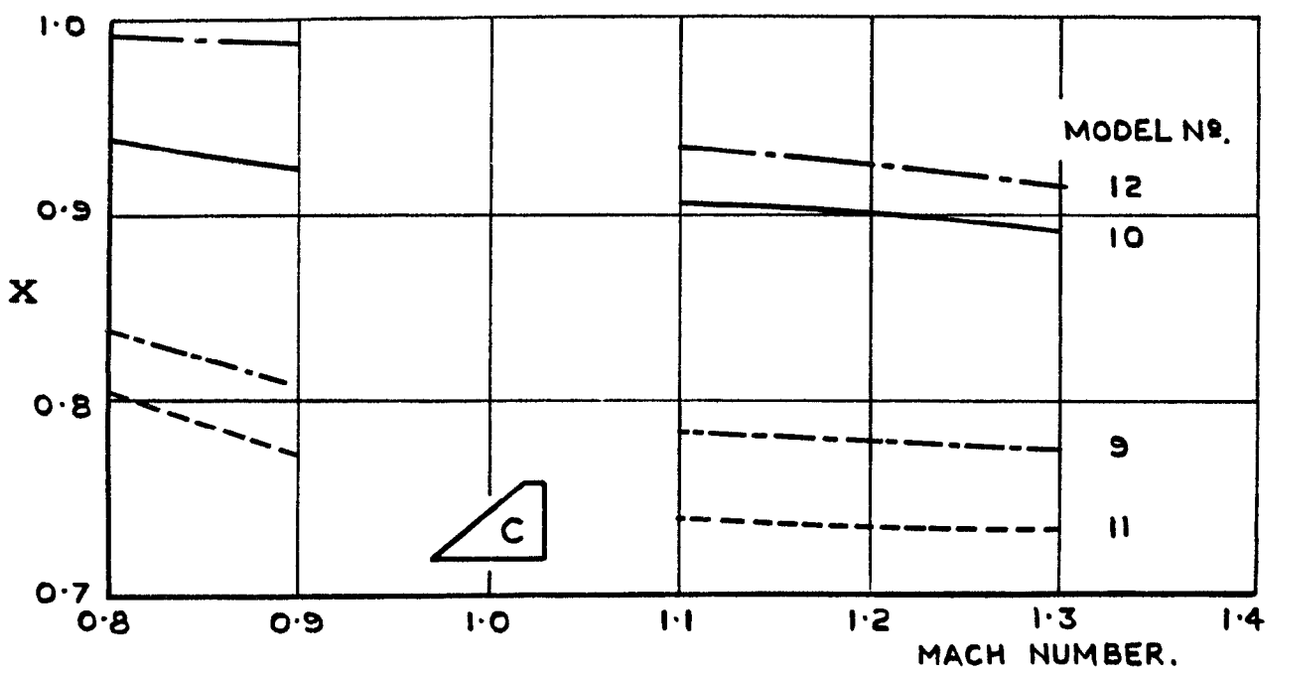

PLANFORM C

FIG. 12. AEROELASTIC CORRECTIONS.

A.R.C. C.P. No. 572

533.694.51 :
533.693.1 :
533.692.1 :

FREE-FLIGHT MEASUREMENTS OF CONTROL EFFECTIVENESS ON THREE WING PLANFORMS AT TRANSONIC SPEEDS. 533.6.011.35 :
533.6.055 :
Edwards, J.B.W. March 1961. [Ae] RAE 102

The rolling effectiveness of a series of flap and tip controls has been measured by means of rocket-propelled test vehicles, over the Mach number range 0.8-1.3. The controls were attached to three basic planforms all of nett aspect ratio 2.83 and having R.A.E. 102 aerofoil sections. Each planform was flown with four different controls and two values of thickness:chord ratio (0.06 and 0.075).

Results for all the configurations are given in terms of the ratio ℓ_ξ/ℓ_p: for certain wing:control combinations it was possible to isolate the aileron-effectiveness derivative ℓ_ξ.

A.R.C. C.P. No. 572

533.694.51 :
533.693.1 :
533.692.1 :

FREE-FLIGHT MEASUREMENTS OF CONTROL EFFECTIVENESS ON THREE WING PLANFORMS AT TRANSONIC SPEEDS. 533.6.011.35 :
533.6.055 :
Edwards, J.B.W. March 1961. [Ae] RAE 102

The rolling effectiveness of a series of flap and tip controls has been measured by means of rocket-propelled test vehicles, over the Mach number range 0.8-1.3. The controls were attached to three basic planforms all of nett aspect ratio 2.83 and having R.A.E. 102 aerofoil sections. Each planform was flown with four different controls and two values of thickness:chord ratio (0.06 and 0.075).

Results for all the configurations are given in terms of the ratio ℓ_ξ/ℓ_p: for certain wing:control combinations it was possible to isolate the aileron-effectiveness derivative ℓ_ξ.

A.R.C. C.P. No. 572

533.694.51 :
533.693.1 :
533.692.1 :

FREE-FLIGHT MEASUREMENTS OF CONTROL EFFECTIVENESS ON THREE WING PLANFORMS AT TRANSONIC SPEEDS. 533.6.011.35 :
533.6.055 :
Edwards, J.B.W. March 1961. [Ae] RAE 102

The rolling effectiveness of a series of flap and tip controls has been measured by means of rocket-propelled test vehicles, over the Mach number range 0.8-1.3. The controls were attached to three basic planforms all of nett aspect ratio 2.83 and having R.A.E. 102 aerofoil sections. Each planform was flown with four different controls and two values of thickness:chord ratio (0.06 and 0.075).

Results for all the configurations are given in terms of the ratio ℓ_ξ/ℓ_p: for certain wing:control combinations it was possible to isolate the aileron-effectiveness derivative ℓ_ξ.

Published by
HER MAJESTY'S STATIONERY OFFICE

To be purchased from
York House, Kingsway, London W.C.2
423 Oxford Street, London W.1
13A Castle Street, Edinburgh 2
109 St. Mary Street, Cardiff
39 King Street, Manchester 2
50 Fairfax Street, Bristol 1
2 Edmund Street, Birmingham 3
80 Chichester Street, Belfast 1
or through any bookseller

Printed in England

S.O. CODE No.23-9012-72